Hindawi
Mathematical Problems in Engineering
Volume 2023, Article ID 3443699, 8 pages
https://doi.org/10.1155/2023/3443699

Research Article

Simplified Calculation of Lateral Displacement of a Cement-Soil Gravity Retaining Wall

Shiwei Qin, Li Wei, and Zili Dai

Department of Civil Engineering, Shanghai University, Shanghai 200444, China

Correspondence should be addressed to Zili Dai; zilidai@shu.edu.cn

Received 11 May 2022; Revised 5 July 2022; Accepted 8 July 2022; Published 14 April 2023

Academic Editor: Naeem Jan

A common retaining structure in Shanghai's soft soil foundation pit is the cement-soil gravity retaining wall. In this research, a streamlined calculation method is suggested to examine the lateral displacement of the cement-soil gravity retaining wall's deformation features. First, the lateral pressure of the retaining wall in a nonlimit passive state is calculated by separately estimating water and soil pressure. Then, the work performed by the lateral pressure of the retaining wall and the internal energy of deformation is calculated and analyzed according to the law of energy conservation to obtain the maximum lateral displacement at the top of the retaining wall. At last, the influences of wall insertion ratio, wall width, cement mixing ratio, and soil internal friction angle on the lateral displacement of retaining wall are analyzed with finite element numerical simulation. The results of the streamlined calculations are contrasted with the measured findings when paired with engineering scenarios, which demonstrates that the predicted lateral displacement is reasonably accurate with an average error of less than 15%.

1. Introduction

With the accelerated urbanization in China, supertall buildings with deep foundations become the mainstream of urban construction. Gravity cement-soil wall, a gravity support structure of grids or solids overlapped by cement-soil piles, is commonly used in deep foundation pit in soft soil areas such as Shanghai, China, because of its convenience and economy [1]. Predicting its lateral displacement is an important part of foundation pit engineering design.

Over the years, general research works have been carried out on the mechanism and prediction of foundation pit deformation, and significant academic achievements and outstanding technical and economic benefits have been obtained. For example, Sadrekarimi [2] carried out pseudostatic limit equilibrium analyses to compare the external and internal stability of gravity retaining walls subject to static and seismic loading conditions, and investigated the possibility of improving the seismic performance. Li et al. [3] offered a new approach to consider the seismic stability of gravity retaining walls based on the category of the upper bound theorem of limit analysis. Yang [4] introduced a computation method of retaining wall reliability indexes and established an analysis model of gravity retaining wall reliability. Chen et al. [5] simulated the lateral earth pressure, the stress distributions, and the forces of the reinforcements in a retaining wall using a three-dimensional finite element model. The simulation results were in good agreement with the field observation data. Guha Ray and Baidya [6] analyzed the reliability of a gravity retaining wall and quantified the uncertainties of the geotechnical random variables based on a pseudodynamic method. Fleischer et al. [7] analyzed the stability of the gravity retaining walls using a two-dimensional FE model taking into account the interaction between crack formation and distribution of the inner water pressure. Ahmed and Basha [8] proposed a wedge failure mechanism to determine active earth pressure exerted on gravity retaining walls and analyzed the external stability. Most of the available research studies focused on the stability and reliability of gravity retaining walls based on the finite element method and the pseudostatic limit equilibrium method, but the calculation method of the lateral deformation of the gravity retaining walls is less on relative

publications, though it is of great importance for the rational design of the deep foundation pit.

Based on the deformation characteristic curves formed by the monitoring data on site, a simplified calculation method is proposed in this study to predict the lateral displacement of the cement-soil gravity retaining structure in mucky clay layer according to the energy conservation law. The relations between the lateral displacement of the retaining structure with the pile rigidity and excavation depth are established, and the reliability of the simplified method is verified combined with the project cases in Shanghai, China.

The proposed technique was used in Shanghai, China, to forecast the lateral displacement of the retaining walls in the foundation pit engineering. Through comparison between the outcomes of the FEM and the measured data collected on site, the applicability and accuracy of the suggested technique were confirmed.

The rest of this study arrangements are as follows: Section 2 analyzes the features of lateral displacement. Section 3 explains the simplified calculation of lateral displacement. Section 4 evaluates the verification of the simplified calculation method. Section 5 discusses the engineering case analysis. Section 6 concludes the study.

2. Features of Lateral Displacement

On-site monitoring data of the lateral displacement of the gravity retaining walls are obtained in a large number of engineering cases in Shanghai, China. By curve fitting, the basic displacement curve along the vertical direction of the gravity retaining wall is as shown in Figure 1 and can be explained as follows:

$$\delta(z) = B_m\left(1 + \cos\frac{\pi}{H}z\right), \tag{1}$$

where $\delta(z)$ is the lateral displacement of the retaining wall along the z direction,H is the retaining wall height, and B_m is the dimensionless coefficient.

It can be seen from Figure 1 that the lateral deformation characteristics of the cement-soil gravity retaining wall can be concluded as follows:

(1) The lateral displacement of the retaining wall presents a half-cycle cosine function, in which the lateral displacement gradually decreases with the increase in the wall depth.

(2) The maximum lateral displacement arises at the top of the retaining wall ($z = 0$) with the maximum displacement of 2Bm, and the minimum displacement occurs at the bottom of the retaining wall ($z = H$).

3. Simplified Calculation of Lateral Displacement

According to the Shanghai.Code for investigation of geotechnical engineering (DGJ08-37-2012), a mucky clay layer of 12~18 m is generally distributed within 20 m below the ground surface of the Shanghai area, and the pile length of the cement-soil gravity retaining wall is generally 9~16 m.Therefore, in this study, the cement-soil gravity retaining wall in the mucky clay in Shanghai is the reference object of this research.

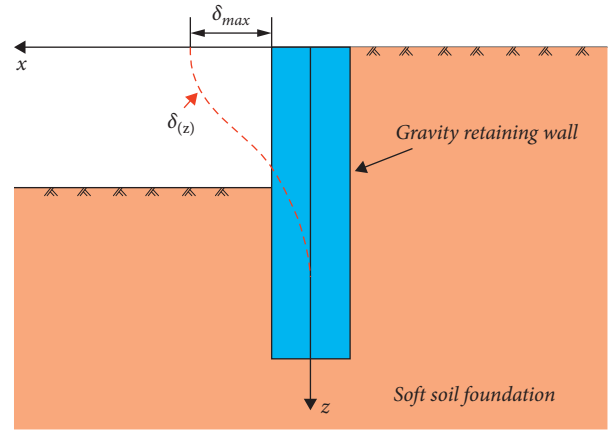

Figure 1: Lateral displacement characteristics of a gravity retaining wall.

3.1. Calculation Assumptions

(a) The cement-soil gravity retaining wall with a length of H, a width of B, and a thickness of 1 m is analyzed as the research object, which can be regarded as a vertically placed beam.

(1) is the functional expression of the lateral displacement along the vertical direction. As shown in Figure 2, h is the excavation depth of the foundation pit on the passive side of the retaining wall, D is the embedded depth of the retaining wall below the excavation surface, and a and b are the distances of the stable groundwater level to the ground and excavation surface from the active side and passive side, respectively.

(b) The cement-soil gravity retaining structure is regarded as an elastic body. Its deformation under the external force is within an allowable deformation range. The force and displacement are linearly related, which conforms to Hooke's law.

(c) The pressure on both sides of the cement-soil retaining wall shall be calculated by separately estimating the water and Earth pressure. The Earth pressure of the active side and passive side shall be calculated according to the static soil pressure and soil pressure under a nonlimit state, respectively, and the water pressure shall be estimated according to the triangular distribution.

(d) If the bottom end of the retaining wall is assumed to be a fixed end and the displacement due to the wall weight is ignored, the retaining wall will transversely bend under lateral pressure, without rigid displacement.

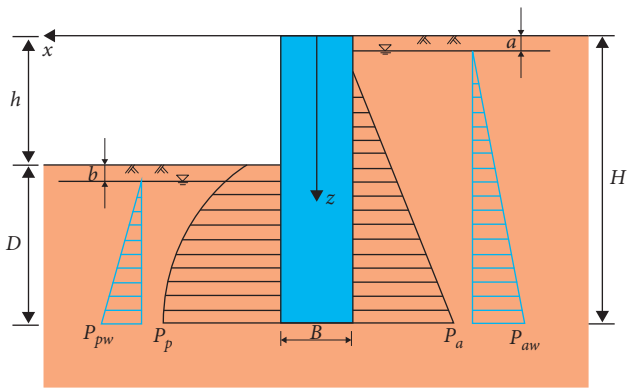

FIGURE 2: Schematic diagram of side pressure calculation of retaining wall.

(e) The soil around the retaining wall is simplified as a homogeneous soil layer during the displacement calculation. The soil parameters can be weighted by the corresponding thickness of each soil layer within the calculation depth range, and the average value is taken.

3.2. Calculation of Lateral Pressure Distribution on the Retaining Wall. The distribution and magnitude of the soil pressure are related to the deformation of the retaining wall. According to the Shanghai technical code for excavation engineering (DGJ08-37-2012), the lateral pressure on the cement-soil gravity retaining wall shall be calculated by separately estimating the water and soil pressure. When strictly limiting the lateral displacement of the retaining structure, the static soil pressure shall be adopted, or the active soil pressure value shall be increased. In a limit equilibrium, the Earth pressures on the active and passive sides of the retaining wall are linearly distributed in a triangle and trapezoid, respectively, as shown in Figure 2. However, during the excavation of foundation pits, the displacement of the soil in the limit equilibrium, especially in the passive limit equilibrium, often does not meet the deformation requirements [9]. It is difficult for the Earth pressure on the passive side of the retaining wall to reach limit equilibrium due to soil stress redistribution and slight deformation caused by the foundation pit excavation. So the practical construction is often in a nonlimit state. To calculate the soil pressure under a nonlimit state, Chen et al. [9] proposed the relationship between soil pressure and displacement on the retaining structure by a quasiexponential function, and the influence of cohesion c is considered. Therefore, in this study, considering the deformation limit of the foundation pit, when calculating the lateral displacement of the cement-soil gravity retaining structure, the active Earth pressure on the wall is calculated using the static Earth pressure. In contrast, the passive Earth pressure is calculated using the Earth pressure under the nonlimit state. At the same time, the water and soil pressures on the active side of the retaining wall are separately calculated. The water pressure on both sides is distributed in a triangle below the groundwater level, as shown in Figure 2.

3.2.1. Calculation of Earth Pressure on Both Sides of the Retaining Structure. The active earth pressure on the retaining wall is calculated using the static soil pressure as follows:

$$p_a = \gamma z K_0, \tag{2}$$

where p_a and γ are the static soil pressure and the unit weight of soil on the active side, respectively. z is the thickness of the soil below the ground surface. K_0 is the static soil pressure coefficient. Since the soil discussed in this study is mucky clay, the value can be taken by

$$K_0 = 0.95 - \sin\varphi', \tag{3}$$

where φ' is the effective internal friction angle measured by the triaxial consolidated undrained shear test, and the weighted average value is taken for layered soils.

The passive-side soil pressure of the retaining wall is calculated using the soil pressure in the following nonlimit state:

$$p_P = p_0 + \left(p_{\text{pcr}} - p_0\right)\left(\frac{\delta}{\delta_{pcr}}\right)e^{\alpha\left[1-\left(\delta/\delta_{\text{pcr}}\right)\right]}, \tag{4}$$

where p_p is the passive Earth pressure; p_0 is the static Earth pressure, which can be valued giving to equation (5); p_{pcr} is the passive soil pressure under limit equilibrium, which can be valued giving to equation (6); δ is the lateral displacement of the retaining structure; δ_{pcr} is the displacement caused by the passive soil pressure of the retaining structure in limit equilibrium, and $\delta_{\text{pcr}} = \text{nD}$; n is the empirical coefficient, and the value is between 0.01 and 0.1; D is the fixed depth of the retaining wall; and α is a parameter related to soil properties, and $0 \le \alpha \le 1$.

$$p_0 = \gamma(z - h)K_0, \tag{5}$$

where h represents the excavation depth on the passive side of the retaining wall; b is the distance from the excavation surface to the groundwater level on the passive side.

$$p_{\text{pcr}} = \gamma(z - h)K_p + 2c\sqrt{K_p}, \tag{6}$$

where K_p represents the passive soil pressure coefficient on the passive side of the retaining structure, $K_p = \tan^2(45^\circ + \varphi/2)$; c is the soil cohesion; and the weighted average value is taken when the soil is layered soil.

3.2.2. Calculation of Water Pressure on Both Sides of Retaining Wall. The active-side water pressure of the retaining wall is as follows:

$$p_{aw} = \gamma_w(z - a), \tag{7}$$

where γ_w is the unit weight of groundwater; a is the distance from the ground line on the active side of the retaining wall to the groundwater level.

The passive-side water pressure of the retaining wall is as follows:

$$p_{pw} = \gamma_w (z - h - b). \tag{8}$$

3.3. Work Calculation of Earth and Water Pressure

3.3.1. Work Calculation of Earth Pressure. The work performed by the Earth pressure on both sides of the retaining structure is the product of the work performed by the active soil pressure and the passive Earth pressure.

The result of the static Earth pressure on the active side and the lateral displacement of the wall along the retaining wall's depth direction is the work produced by the active Earth pressure. Combining equations (1) and (2), the integral will be as follows:

$$\begin{aligned} W_a &= \int_H p_a \delta(z) \mathrm{d}z \\ &= \int_H B_m \left(1 + \cos\frac{\pi}{H} z\right) \gamma z K_0 \mathrm{d}z \\ &= B_m K_0 \gamma H^2 \left(\frac{1}{2} - \frac{2}{\pi^2}\right). \end{aligned} \tag{9}$$

The work done by the passive Earth pressure is the integral of the product of the Earth pressure on the passive side and the lateral displacement of the wall along the depth direction of the retaining wall. Combining equations (1) and (4)~(6), the integral can be expressed as follows:

$$\begin{aligned} W_p &= \int_D p_P \delta(z) \mathrm{d}z \\ &= \int_h^H \Big\{ \gamma (z - h) K_0 + \Big[\gamma (z - h) K_p \\ &\quad + 2c\sqrt{K_p} - \gamma (z - h) K_0 \Big] \cdot \left(\frac{\delta}{\delta_{\mathrm{pcr}}}\right) e^{\alpha \left[1 - \left(\delta / \delta_{\mathrm{pcr}}\right)\right]} \Big\} \delta(z) \mathrm{d}z. \end{aligned} \tag{10}$$

3.3.2. Work Calculation of Water Pressure. The work done by the water pressure is the sum of the work done by the water pressure on both active and passive sides of the retaining wall.

The work done by the water pressure on the active side of the wall is the integral of the product of the lateral displacement of the wall along the depth direction and the active-side water pressure, which can be expressed as follows:

$$\begin{aligned} W_{aw} &= \int_a^H p_{aw} \delta(z) \mathrm{d}z \\ &= \int_a^H \gamma_w (z - a) B_m \left(1 + \cos\frac{\pi}{H} z\right) \mathrm{d}z \\ &= \gamma_w B_m \left(\frac{1}{2} H^2 - Ha + \frac{1}{2} a^2 - \frac{H^2}{\pi^2} - \frac{H^2}{\pi^2} \cos\frac{\pi}{H} a\right). \end{aligned} \tag{11}$$

The work done by the passive-side water pressure is the integral of the product of the lateral displacement of the wall along the depth direction and the passive-side water, which can be expressed as follows:

$$\begin{aligned} W_{pw} &= \int_{h+b}^H p_{aw} \delta(z) \mathrm{d}z \\ &= \int_{h+b}^H \gamma_w (z - h - b) B_m \left(1 + \cos\frac{\pi}{H} z\right) \mathrm{d}z \\ &= \gamma_w B_m \left[\frac{1}{2} H^2 - \frac{H^2}{\pi^2} - H(h + b) \right. \\ &\quad \left. + \frac{1}{2} (h + b)^2 - \frac{H^2}{\pi^2} \cos\frac{\pi (h + b)}{H}\right]. \end{aligned} \tag{12}$$

3.4. Deformation of Internal Energy Calculation of Retaining Wall. For the small displacement caused by the weight of the cement-soil gravity retaining wall, the compressing strain energy caused by weight shall be ignored. However, the retaining wall is regarded as a vertically placed elastic beam of which certain lateral displacement occurs. Then, the elastic deflection distortion of the beam under water and soil pressure accumulates bending strain energy and shear strain energy. Since the shear deformation has little effect on the beam displacement, the shear strain energy is generally ignored, so the bending strain energy is the deformation internal energy generated during the elastic deformation of the retaining wall. According to the known lateral deformation relation, the calculation of the shear strain energy is as follows:

$$\begin{aligned} V_\varepsilon &= \int_H \frac{1}{2} EI \left[\frac{d^2 \delta(z)}{dz^2}\right]^2 \mathrm{d}z \\ &= \int_0^H \frac{1}{2} EI \left\{\frac{d^2 \left[B_m{}^2 (1 + \cos\pi / Hz)^2\right]}{dz^2}\right\}^2 \mathrm{d}z \\ &= \frac{B_m{}^2 EI \pi^4}{4H^3}. \end{aligned} \tag{13}$$

3.5. Solution Based on the Principle of Energy Conservation. When a deformable solid deformed under an external force, the work done on the corresponding displacement is equivalent to the strain energy in the object. According to the principle of energy conservation, the work done by the external force of the cement-soil gravity retaining wall is converted into its strain energy. Therefore, regarding the cement-soil gravity retaining wall as a system, the work done by the water and soil pressure on the external force is equal to the sum of the strain energy of the retaining wall, that is,

$$W_a + W_{aw} - W_p - W_{pw} = V_\varepsilon. \tag{14}$$

We bring equations (9)–(13) into the above equation to obtain the coefficient B_m; then, the lateral deformation curve

Table 1: Physical and mechanical properties of soil.

No.	Soil types	Thickness h (m)	Unit weight γ (kN/m^3)	Cohesion c (kPa)	Internal friction angle φ (°)
1	Miscellaneous fill	1.055			
2	Silty clay	2.244	18.61	12.1	16.30
3	Mucky clay	12.471	16.62	14.0	12.51
4	Clay	1.431	17.90	13.2	13.50
5	Silty clay mixed with silt	7.272	18.33	14.1	17.55

of the retaining wall and the maximum displacement $2B_m$ at the wall top can be obtained.

4. Verification of the Simplified Calculation Method

To verify the applicability and accuracy of the simplified calculation method proposed in this work, a foundation pit engineering in Shanghai, China, is selected as a case study to compare the lateral deformation of the gravity retaining wall obtained through the simplified calculation method and the finite element method (FEM).

4.1. Project Overview. Taking the auxiliary housing project in Songjiang District, Shanghai, as an example, the foundation pit is 110 m long and 36 m wide, with an excavation depth of 6 m, a circumference of about 371 m, and an excavation area of about 7893 m^2. The retaining structure adopts the cement-soil gravity retaining wall, with a cement mixing ratio of 10%, a wall pile length of 12 m, and a wall width of 3.7 m.

The soil layers in the foundation pit site mainly include from top to bottom: miscellaneous fill, silty clay, mucky clay, clay, and silty clay mixed with silty sand. The soil layer within the depth range of the retaining wall is mainly mucky clay. The physical and mechanical properties of each soil layer are shown in Table 1.

4.2. Model Establishment. A two-dimensional FEM model is established for the section of the foundation pit. The foundation pit's symmetry makes it possible to take half of the foundation pit along the excavation width direction for analysis. To eliminate the influence of the boundary effect, the excavation depth of the soil behind the retaining wall is about six times in the horizontal direction and five times in the vertical direction, so the size of the soil model is 155 m × 30 m.

The plane strain calculation model is accepted, and the Mohr-Coulomb constitutive model is used for the soil material. The retaining wall is regarded as isotropic; the initial stress field is considered the self-weight stress field; and the material parameters are taken according to Table 1. The automatic mesh division is employed for the mesh while calculating. Before dividing the mesh, the model's size shall be controlled, with the soil mesh size of 2 and the retaining wall's mesh size of 1. Figure 3 shows the calculation model.

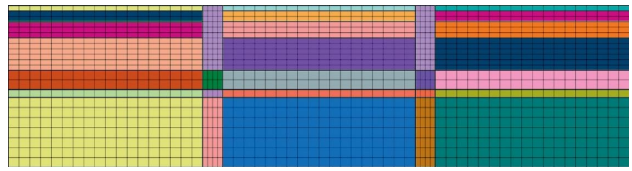

Figure 3: Finite element mesh model.

4.3. Calculation of Working Conditions. Four groups of working conditions are set up for the calculation. The lateral displacement changes under the four working conditions of different insertion ratios, wall widths, excavation depths, and mixing ratios of cement-soil are analyzed, respectively. The specific settings of the working conditions are as follows:

Control group: the wall insertion ratio is 1.0, the wall width is 3.7 m, the excavation depth is 6 m, and the cement mixing ratio is 10%;

Working condition 1: the wall insertion ratio is 0.6, 0.8, 1.0, 1.2, and 1.4; and other parameters are the same as the control group;

Working condition 2: the wall width is 2.7 m, 3.2 m, 3.7 m, 4.2 m, and 4.7 m; and other parameters are the same as the control group;

Working condition 3: the mixing ratio of wall cement is 10%, 12.5%, 15%, 17.5%, and 20%; and other parameters are the same as the control group;

Working condition 4: the internal friction angle of the soil is 11°, 13°, 15°, 17°, and 19°; and other parameters are the same as the control group.

4.4. Analysis of Calculation Results

4.4.1. Influence of Wall Insertion Ratio on Lateral Displacement. The same total length of the retaining wall and different excavation depths of the foundation pit are used to simulate the influence of different insertion ratios on the lateral displacement of the wall. The numerical simulation results and theoretical calculation results are shown in Figure 4.

It can be seen from Figure 4 that the theoretical calculation results and the numerical simulation results show the same change trend. The lateral displacement at the top of the retaining wall increases with the excavation depth and decreases with the increase in the wall insertion ratio. Therefore, strict control of the excavation depth and real-time monitoring of the lateral displacement of the retaining wall can prevent excessive deformation. At the same time, the wall insertion ratio can be appropriately increased within the allowable design range, which can also limit the deformation.

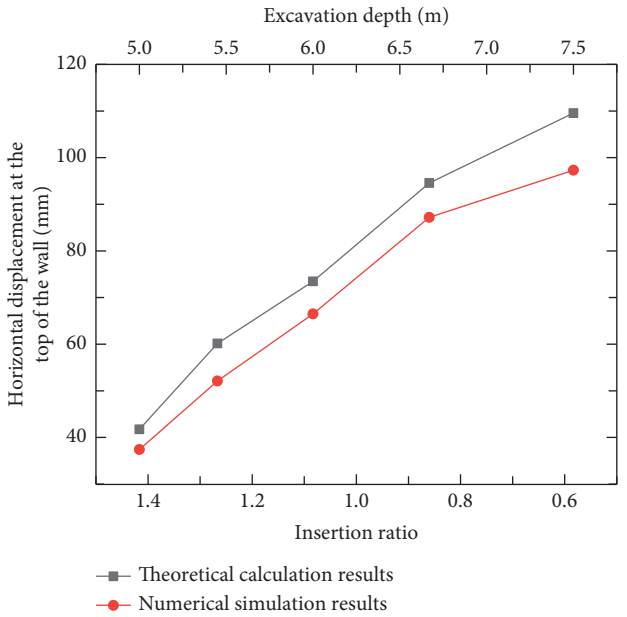

Figure 4: Relationship between wall insertion ratio (excavation depth) and wall top lateral displacement.

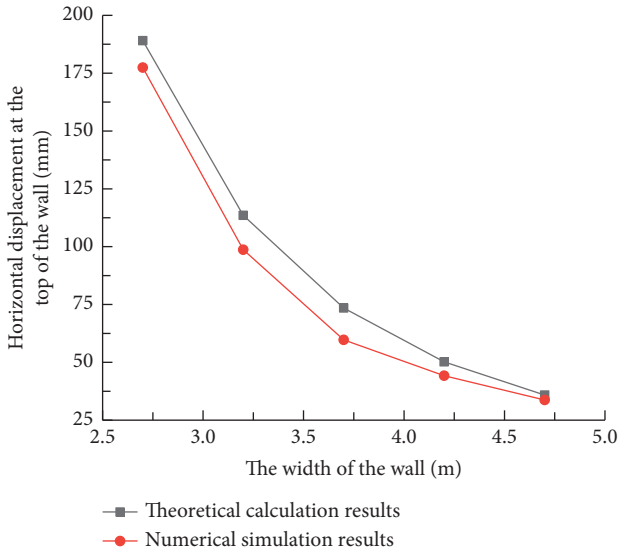

Figure 5: Relationship between the wall width and wall top lateral displacement.

4.4.2. Influence of Wall Width on Lateral Displacement. When excavated to the bottom of the pit, the lateral displacement change of the top of the retaining wall with different wall widths is analyzed, as shown in Figure 5.

It can be seen from the figure that the lateral displacement of the wall top decreases with the increase in the wall width, and the decreasing rate is gradually slow. The theoretical calculation results are consistent with the numerical simulation results. When the wall width increases from 2.7 m to 3.2 m, the lateral displacement of the wall top is reduced by 75.49 mm with a large reduction, and then, for each increase of 0.5 m. Compared with the previous stage,

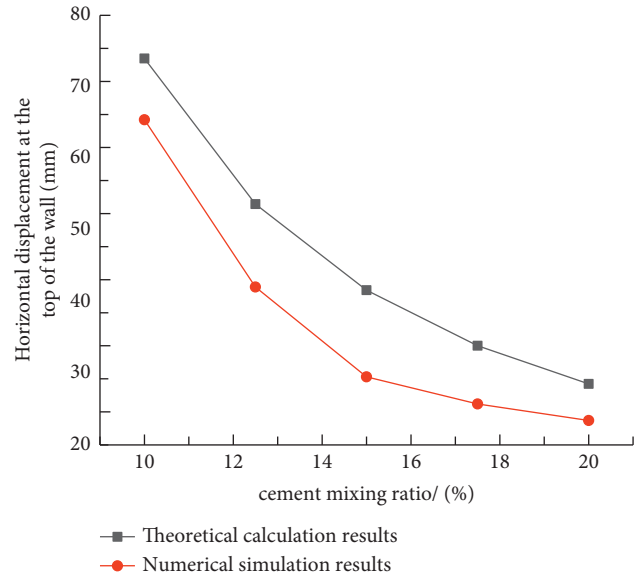

Figure 6: Relationship between cement mixing ratio and wall top lateral displacement.

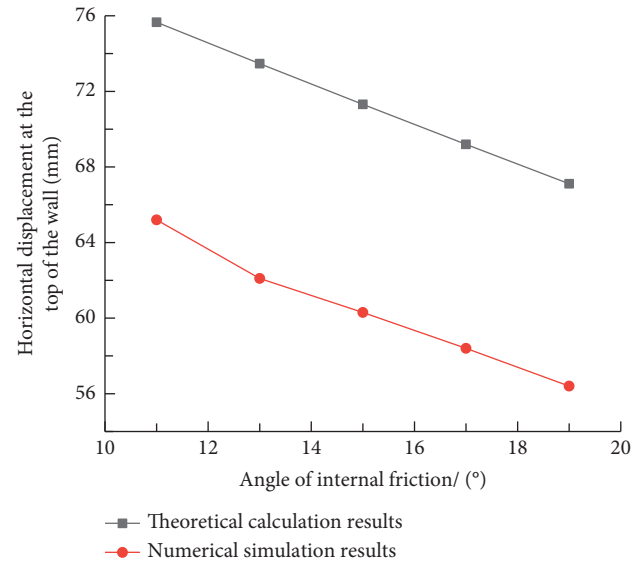

Figure 7: Relationship between internal friction angle and lateral displacement of wall top.

the lateral displacement of the top of the wall is reduced by 40.1 mm, 23.24 mm, and 14.38 mm, respectively; and the reduction is smaller and smaller. The moment of inertia I of the wall also grows with the increases in wall width. With the increase in wall rigidity, the deformation under external force can be controlled. The width of the wall exceeds 3.7 m, making it difficult for the wall to have lateral displacement. Therefore, this project is reasonable for the retaining wall to be 3.7 m wide.

4.4.3. Influence of Cement Mixing Ratio on Lateral Displacement. According to the Handbook of Foundation Treatment [10], when the cement mixing ratio of cement-soil

Table 2: Comparison of measured values and theoretically calculated values of each engineering case.

No.	Project name	Wall length/m	Wall width/m	Excavation depth/m	Lateral displacement of wall top/mm		Error/%
					Calculating results	Measured data	
1	Foundation pit in Hou et al. (2014) [11]	13.5	4.7	5.65	82.3	71	15.9
2	Kangji building in Chen et al. (1997) [12]	12.0	4.2	5.95	40.6	35	16.0
3	Water company in Ding et al. (2005) [13]	15.3	3.7	6.3	33.1	24	9.1
4	Foundation pit in Gong (2008) [10]	9.2	3.2	4.8	29.4	26	13.1
5	Port authority building in Li et al. (1998) [14]	9.0	3.2	5	35.7	40	10.75
6	Foundation pit in Xiong (2003) [15]	13.3	5.3	6.2	96.2	82	17.3

gravity retaining wall is 10% ~ 20%, the relationship between unconfined compressive strength of cement soil and cement mixing ratio can be expressed as follows:

$$\frac{q_{u1}}{q_{u2}} = \left(\frac{a_{w1}}{a_{w2}}\right)^{1.6}, \tag{15}$$

where q_{u1} and q_{u2} are the unconfined compressive strengths with cement mixing ratios of a_{w1} and a_{w2}, respectively.

When the cement content is 10%, the unconfined compressive strength qu of cement-soil is 1 MPa. If qu1 = 1 MPa and aw1 = 10% in equation (15), the calculated cement content a_{w2} is 12.5%, 15%, 17.5%, and 20%; and the corresponding unconfined compressive strength of soil-cement is 1.429 MPa, 1.91 MPa, 2.448 MPa, and 3.03 MPa. Since the deformation modulus E of cement-soil is generally 120 to 150 times the unconfined compressive strength, the deformation modulus of cement-soil with cement mixing ratios of 10%, 12.5%, 15%, 17.5%, and 20% conservatively takes 120 MPa, 171.49 MPa, 229.57 MPa, 293.81 MPa, and 363.77 MPa.

The effect of the cement mixing ratio on the lateral displacement is investigated by altering the deformation modulus of the cement-soil retaining wall. Figure 6 displays the outcomes of the numerical simulation and the theoretical computation. It can be seen from the figure that with the increase in the cement mixing ratio, the lateral displacement of the wall top gets smaller and smaller, and the deceleration gets slower and slower. When increasing the mixing ratio from 10% to 12.5%, it can be seen that the lateral displacement of the wall top greatly decreases. When increasing the mixing ratio from 12.5% to 15%, it can be noted that the lateral displacement of the wall top significantly decreases. However, when increasing the mixing ratio from 15% to 17.5% and from 17.5% to 20%, we can see that the decrease in the lateral displacement of the wall top is relatively limited. Therefore, increasing the cement mixing ratio can improve the rigidity of the wall to control lateral deformation. In addition, the variation in the figure is similar to the influence law of increasing the wall width on lateral displacement because increasing the wall width and cement mixing ratio will improve the flexural rigidity EI of the cement-soil retaining wall.

4.4.4. Influence of Soil Internal Friction Angle on Lateral Displacement. The soil layer within the depth of the retaining wall of the project is mainly composed of mucky clay. The internal friction angle of this soil layer in Shanghai is between 9.5° and 19.5°. So the internal friction angle of the soil layer is set as 11°, 13°, 15°, 17°, and 19° to analyze the influence of different internal friction angles on the lateral displacement of the wall top, as shown in Figure 7.

It can be seen from the figure that the lateral displacement variation of the wall top by theoretical calculation is consistent with the numerical simulation results, which shows a decreasing trend with the increase in the soil internal friction angle, with obvious linear variation characteristics. However, the reduction is not large. When increasing the internal friction angle by 1°, we get a lateral displacement of the wall top that decreases by about 1 mm. Compared with the increase in the wall insertion ratio and the wall width, increasing the soil internal friction angle has a minimal influence on the lateral displacement of the wall top.

5. Engineering Case Analysis

The lateral deformation of the cement-soil gravity retaining walls in six foundation pit engineering cases in Shanghai is calculated using the simplified method. The calculated results are compared with the measured data in situ to verify the applicability of the proposed calculation method. The calculation errors are shown in Table 2. It shows that the simplified calculation results of each engineering case are relatively close to the measured results, with a maximum error of 17.3%, a minimum error of 9.1%, and an average error of 13.69%. For the foundation pit projects using the cement-soil gravity retaining walls as the retaining structure in the mucky clay area in Shanghai, the method can predict the lateral displacement of the retaining walls, which provides a reference for the engineering design.

6. Conclusions

This study used the separated calculation of water and Earth pressure theory to investigate the deformation features of a cement-soil gravity retaining wall while taking into account the nonlimit state of the passive-side soil pressure. Based on the energy conservation law, a simplified calculation method for the lateral displacement of the cement-soil gravity retaining wall was then proposed. The proposed method was applied to predict the lateral displacement of the retaining walls in the foundation pit engineering in Shanghai, China.

The applicability and accuracy of the proposed method were verified through the comparison with the FEM results and measured data in situ. The following conclusions are drawn as follows:

(1) The calculation method considers the influence of the cement mixing ratio, cross-sectional area, excavation depth, and embedded depth of the cement-soil retaining wall on the lateral displacement, which is more comprehensive. The prediction accuracy is close to the lateral deformation of the retaining wall measured in situ.

(2) Elastic deflection deformation is what gives the retaining wall its lateral displacement. At the top of the wall, the displacement is greatest. By examining the parameters influencing the lateral displacement of the retaining wall, its variation law provided by the simplified calculation method accords well with the numerical simulation results.

(3) The lateral displacement of the cement-soil gravity retaining wall is proportional to the insertion ratio and excavation depth. Therefore, on the premise of meeting the design specifications, the embedded depth of the wall can be appropriately increased to decrease its lateral displacement. At the same time, the displacement shall be monitored in real time to ensure safety when a large excavation area occurs in the foundation pit. In addition, the increase in the wall width and cement mixing ratio improves the flexural rigidity of the retaining wall to control its lateral deformation, so the lateral displacement of the retaining wall is inversely proportional to the wall width and cement mixing ratio. Then, the increase in the soil internal friction angle also reduces the lateral displacement of the retaining wall, but for the mucky clay with the friction angle range of 9.5° to 19.5° in Shanghai, the influence is minimal.

(4) The simplified calculation method proposed in this study is applied to the basis pit engineering in Shanghai, of which the calculated results are not much dissimilar from the measured data, and the average error is within 15%. Therefore, this work can provide a reference for the prediction of the lateral displacement of the gravity retaining walls in similar projects in the future.

Data Availability

The data that support the findings of this study are available from the corresponding author upon reasonable request.

Conflicts of Interest

The authors declare that they have no competing interests.

Acknowledgments

This research was funded by the Shanghai Science and Technology Innovation Action Plan (21DZ1204202).

References

[1] S. Yang, M. Zhang, X. Bai, X. Liu, and C. Zheng, "Experiment investigation on stress characteristics of grouting microsteel pipe piles with cement-soil wall," *Advances in Materials Science and Engineering*, vol. 2020, Article ID 9704589, 10 pages, 2020.

[2] A. Sadrekarimi, "Seismic distress of broken-back gravity retaining walls," *Journal of Geotechnical and Geoenvironmental Engineering*, vol. 143, no. 4, Article ID 04016118, 2016.

[3] X. Li, Y. Wu, and S. He, "Seismic stability analysis of gravity retaining walls," *Soil Dynamics and Earthquake Engineering*, vol. 30, no. 10, pp. 875–878, 2010.

[4] H. M. Yang, "The stability reliability analysis about gravity retaining wall," *Advanced Materials Research*, vol. 250-253, no. 1–4, pp. 2352–2355, 2011.

[5] Q. Chen, L. Wan, R. He, and H. Lai, "Load transfer and stress in a piled gravity retaining wall," *Acta Geotechnica Slovenica*, vol. 7, no. 2, pp. 30–44, 2010.

[6] A. Guha Ray and D. K. Baidya, "Reliability based pseudo-dynamic analysis of gravity retaining walls," *Indian Geotechnical Journal*, vol. 48, no. 1, pp. 575–584, 2018.

[7] H. Fleischer, R. Schlegel, and S. Eckardt, "Standsicherheitsberechnungen an bestehenden gewichtsstützwänden," *Bautechnik*, vol. 97, no. 6, pp. 387–394, 2020.

[8] S. M. Ahmed and B. M. Basha, "External stability analysis of narrow backfilled gravity retaining walls," *Geotechnical & Geological Engineering*, vol. 39, no. 3, pp. 1603–1620, 2020.

[9] K. Chen, M. Wang, Q. Xu, and N. Gong, "Numerical analyses of passive earth pressure on rigid retaining wall," *Chinese Journal of Rock Mechanics and Engineering*, vol. 6, pp. 980–988, 2004.

[10] N. Gong, *Handbook of Foundation Treatment*, China Construction Industry Press, Beijing, China, 2008.

[11] J. Hou, J. He, J. Tang, and Y. Tan, "Application of gravity retaining wall with H-shaped steel in soft soil foundation pit," *Rock and Soil Mechanics*, vol. 35, no. S1, pp. 431–436, 2014.

[12] L. Chen, H. Liu, and M. Guan, "Design of cement-soil foundation pit enclosure," *Underground Engineering and Tunnel*, no. 4, pp. 16–24, 1997.

[13] T. Ding, M. Xu, and H. Li, "Analysis on horizontal displacements of composite retaining structure for wide foundation pit," *Building Science*, vol. 21, no. 2, pp. 76–79, 2005.

[14] W. Li, K. Zhang, and L. Gu, "Applied method in calculating displacement of cement-stabilized soil retaining wall," *Industrial Construction*, vol. 28, no. 5, pp. 9–13, 1998.

[15] H. Xiong, "Analysis of a practical deep-mixing-method retaining wall," *Shanghai Geology*, vol. 1, pp. 36–39, 2003.